

Turning Disaster into Knowledge

**GEOLOGICAL AND GEOTECHNICAL ENGINEERING
RECONNAISSANCE OF THE SEPTEMBER 19, 2022,
MICHUACAN EARTHQUAKE, MEXICO**



Authors (in Alphabetical Order):

Kevin B. Clahan, *Letitis Consultants International, Inc., Concord, CA*
Daniel De La Rosa A, *Group of Advance Numerical Modeling and Instrumentation,
Institute of Engineering, National Autonomous University of México, Mexico City*
Juan M. Mayoral V, *Group of Advance Numerical Modeling and Instrumentation from the
Institute of Engineering at National Autonomous University of México*
Mauricio Perez D, *Group of Advance Numerical Modeling and Instrumentation from the
Institute of Engineering at National Autonomous University of México*
Jonathan P. Stewart, *University of California, Los Angeles*

EXECUTIVE SUMMARY

An interface subduction earthquake of moment magnitude 7.7 occurred on September 19, 2022, along the Middle America trench megathrust near the central Pacific coast of Mexico in the state of Michoacan. The earthquake occurred at a relatively shallow depth of 15 km where the Cocos plate is subducting beneath the North America plate. According to the Civil Protection Coordination – the federal agency in charge of leading all activities at the national level to mitigate the effects of natural hazards – there was structural and nonstructural damage in 5,972 houses and 116 schools. Two fatalities occurred due to building collapses in Manzanillo, Colima. An **M**6.9 aftershock occurred on September 22, 2022 and resulted in two additional fatalities. Following the September 19, 2022 event, a joint geotechnical engineering reconnaissance effort was organized between the Group of Advance Numerical Modeling and Instrumentation from the Institute of Engineering at National Autonomous University of México, GEOSIM-IIUNAM, Lettis Consultants International, Inc., and the Geotechnical Extreme Events Reconnaissance Association, GEER, to perform a field reconnaissance of the seismic, geological, and geotechnical issues caused by the September 19, 2022, earthquake. The reconnaissance involved geo-located observations over an 842 km path, with stops at key locations where earthquake effects were observed. These effects included structural damage, roadway and bridge damage, damage to a drainage culvert, and ground failure from liquefaction, lateral spreading, and landsliding. To the extent practical, incidents of ground failure have been mapped so that adjacent areas of non-ground failure can be identified.

ACKNOWLEDGMENTS

The work presented was supported by the Group of Advance Numerical Modeling and Instrumentation from the Institute of Engineering at National Autonomous University of México (GEOSIM-IIUNAM), Lettis Consultants International, Inc., and Geotechnical Extreme Events Reconnaissance Association (GEER). The GEER Association is supported by the U.S. National Science Foundation through the Geotechnical Engineering Program under Grant No. CMMI-1826118. Any opinions, findings, conclusions, or recommendations expressed in this material are those of the authors and do not necessarily reflect the views of the NSF. The GEER Association is made possible by the vision and support of the NSF Geotechnical Engineering Program Directors: Dr. Richard Fragaszy and the late Dr. Cliff Astill. GEER members also donate their time, talent, and resources to collect time-sensitive field observations of the effects of extreme events.

1 INTRODUCTION

An earthquake with a moment magnitude **M**7.7 (SSN, 2022) struck the central region of Michoacan, Mexico on September 19, 2022, at 13:05:09 hours (18:05:09 GMT), about an hour after a national earthquake drill was carried out to prepare for future catastrophic events and commemorate past earthquakes, 1985 and 2017, which also occurred on this same date. The epicenter was located at 18.22 north latitude and -103.29 west longitude according to The National Seismological Service of Mexico (SSN) at a depth of 15 km. This earthquake occurred in Middle America Trench, where the Cocos plate is subducting beneath the North America plate. The mechanism was a reverse faulting. Numerous $M > 7$ earthquakes have occurred along this active stretch of the megathrust plate boundary over the past 50 years, including the **M**8.0, 1985 Michoacan/Mexico City earthquake (History, 2009) which resulted in over 10,000 fatalities (See Figure 1).

The event caused strong ground shaking and damage primarily in the coastal states of Colima and Michoacan, with peak ground accelerations as high as 1g in the epicentral area. In addition, minor damage and moderate shaking were felt in the states of Jalisco, Nayarit, the State of Mexico, and Mexico City. Two fatalities occurred due to building collapses in Manzanillo, Colima. An **M**6.9 aftershock occurred on September 22, 2022, and resulted in an additional two deaths. According to the Civil Protection Coordination – the federal agency in charge of leading at the national level all activities to mitigate the effects of natural hazards – there was structural and nonstructural damage in 5,972 houses and 116 schools. Regarding the health infrastructure, 33 medical units were reported with different levels of damage: one and 32 with severe and minor damage, respectively (CNPC, 2022).

A research team consisting of geotechnical engineers, Daniel de la Rosa and Mauricio Perez, from the Group of Advance Numerical Modeling and Instrumentation from the Institute of Engineering at National Autonomous University of México (GEOSIM-IIUNAM), and Principal Engineering Geologist, Kevin Clahan, from Lettis Consultants International, Inc. (LCI), under the guidance of Juan M. Mayoral (GEOSIM-IIUNAM) and Jonathan Stewart (UCLA), performed a preliminary field investigation of the seismic, geological, and geotechnical issues caused by the September 19, 2022 earthquake.

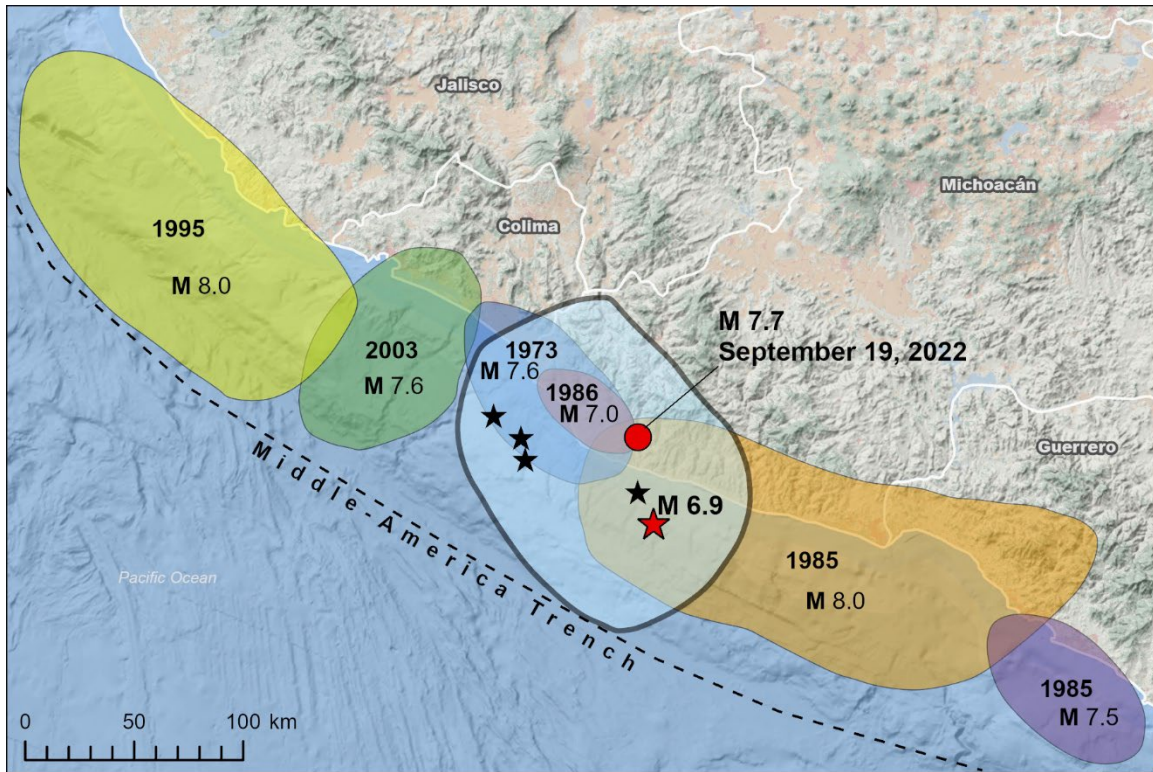


Figure 1. Approximate location of subduction zone rupture planes, west-central Mexico, since 1973. Black stars are 2022 aftershocks $>M5$ (modified from Wartman et al., 2003)

Figure 2 shows the route followed by the research team on September 28-30, 2022, as well as waypoint stations where earthquake related damage or effects were noted. The team used an unmanned aerial vehicle (UAV) to photograph several sites along the route. Table 1 summarizes the damage and effects observed along the route.

This report is based mainly on field reconnaissance from direct observation. Earlier reports on this earthquake including the VERT report (Miranda et al., 2022) are based on reporting and information derived from the internet. The NHERI---DesignSafe Data Depot is being utilized to disseminate digital data collected during this reconnaissance (PRJ-3717, 2022).

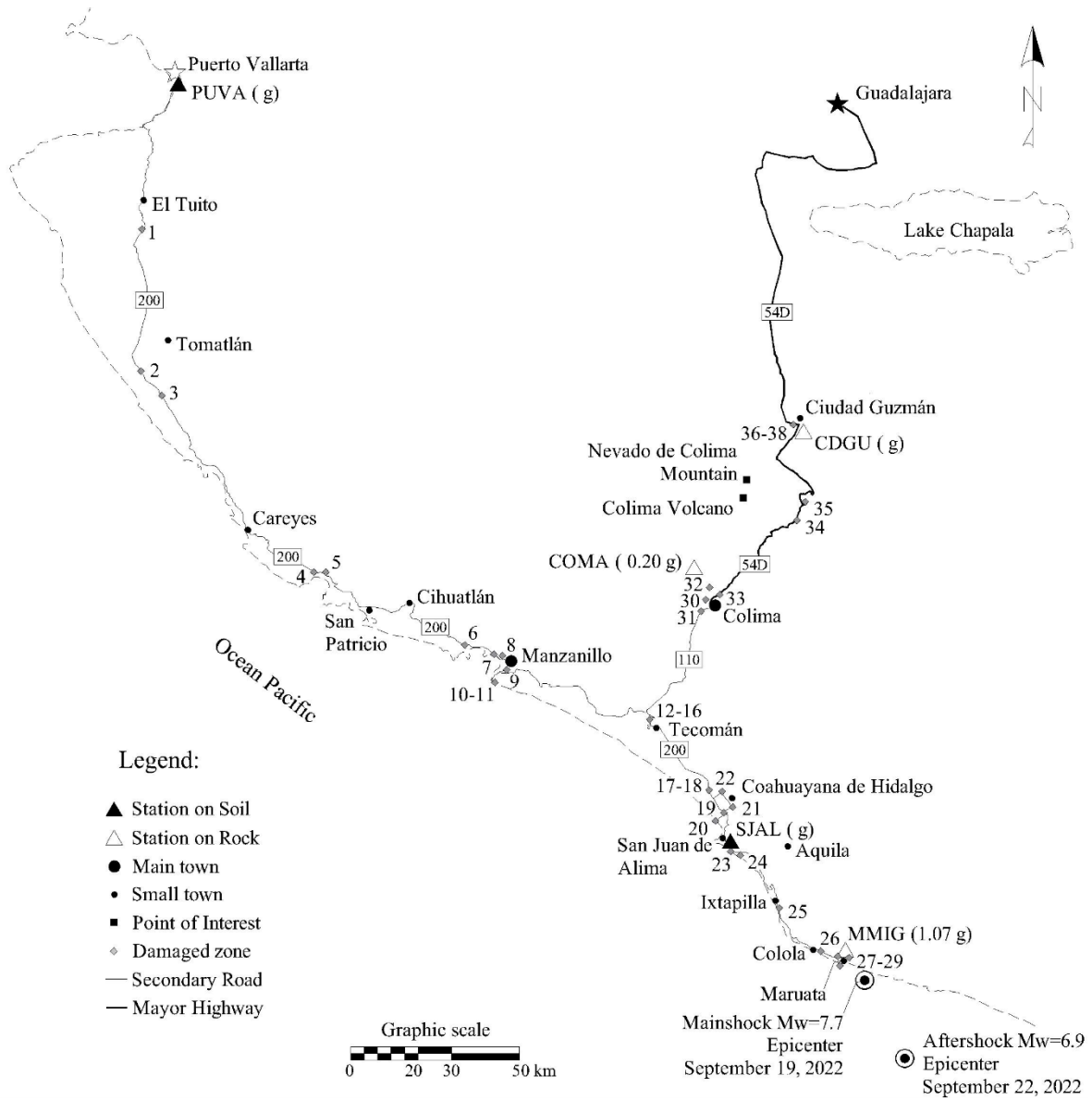


Figure 2. Route followed by the reconnaissance team, numbered waypoint stations, and nearby seismological stations with the value of PGA recorded.

Table 1. Damage observed along reconnaissance route.

Waypoint Station	Coordinates		Damage Summary
	Latitude (°)	Longitude (°)	
1	20.240086	-105.320644	Rockfalls on cut slope along the road
2	19.860358	-105.323112	Rock wedge failure on cut slope along the road
3	19.794496	-105.263413	Gap of joints in decks of the bridge and lateral displacements
4	19.321026	-104.817072	Gap of joints in decks of the bridge
5	19.321026	-104.817072	Vertical cracking in abutment of bridge
6	19.125082	-104.407973	Vertical cracking in abutment of bridge
7	19.100552	-104.325525	Collapse of roof in mall
8	19.095606	-104.302863	Collapse of third floor masonry walls of Coppel store
9	19.058136	-104.290446	Partial collapse of balcony
10	19.024016	-104.322869	Column failures of perimeter walls of school
11	19.024788	-104.323969	Column failure of perimeter walls of thermal power station
12	18.918219	-103.870195	Collapse of perimeter wall of automobile workshop
13	18.911143	-103.871476	Collapse of local grocery store
14	18.910863	-103.871611	Column damage of supermarket
15	18.910531	-103.87186	Damage in door frames and between structures
16	18.910498	-103.87244	Damage to nonstructural elements in church
17	18.724385	-103.722248	Lateral displacements of decks and damage in pier caps of bridge
18	18.717472	-103.716876	Lateral spread feature affecting a road along a natural levee
19	18.670031	-103.681472	Lateral displacements of decks with damage in pier caps of the bridge and rotational failure of abutment
20	18.653076	-103.700458	Lateral spreading in sands due to liquefaction
21	18.684114	-103.669303	Collapse of road culvert made of masonry
22	18.728643	-103.687277	Total collapse of a two-story house with soft first floor
23	18.566463	-103.65394	Multiple rockfalls and landslides on cut slopes along the road
24	18.563754	-103.646552	Landslide and rockfalls along road
25	18.41615	-103.532373	Evidence of liquefaction in riverbed (sand boils)
26	18.298116	-103.412856	Partial collapse of a court cover roof. Structure had evidence of severe rust.
27	18.282195	-103.358294	Severe longitudinal cracking on road due to lateral expansion
28	18.274094	-103.348231	Collapse of masonry walls and damage to structural elements in community hospital and damaged column and wall of nearby masonry two story building

Table 1. Damage observed along reconnaissance route (continuation).

Waypoint Station	Coordinates		Damage Summary
	Latitude (°)	Longitude (°)	
29	18.268759	-103.350911	Lateral spreading and cracking in rural roads due to liquefaction
30	19.243584	-103.728062	Damage and slight cracking in non-structural elements of multiple buildings in the center of the city
31	19.213032	-103.739473	Lateral displacements of decks and damage in pier caps of bridge
32	19.275421	-103.716969	Cracking on non-structural elements with damage on the corner columns
33	19.255976	-103.687608	Vertical cracking in building
34	19.452558	-103.469476	Rockfalls on cut slope along the road
35	19.501861	-103.444079	Rockfalls on cut slope along the road
36	19.709474	-103.467275	Severe damage in three continuous houses with extensive cracking on walls, floor lifting, and tilt of columns
37	19.703666	-103.463191	Roof cracking inside church
38	19.702541	-103.471109	Partial collapse and cracking of perimeter wall of local soccer stadium

2 SEISMOLOGICAL AND GEOLOGICAL OBSERVATIONS

According to the National Seismological Service of México (SSN, 2022), the focus of the seismic event on September 19, 2022, was located at 18.24° north latitude and -103.28° west longitude at a depth of 15 km (Figure 3), with a moment magnitude of **M7.7**, near Coalcoman, Michoacan at 13:05:09 hours (18:05:09 GMT).



Figure 3. Epicenter location (SSN, 2022)

The mechanism of the seismic event corresponds to a reverse faulting, characteristic of earthquakes that occur on or near the plate boundary where the Cocos plate is subducting beneath the North American plate at a rate of approximately 50mm/yr (Figure 4). The September 19, 2022 megathrust earthquake appears to have ruptured a portion of the plate boundary that last ruptured in 1973 in an **M7.6** event (Figure 1). The approximately 50-year gap between the earthquakes is enough time for the fault to reaccumulate significant stress. The 2022 rupture plane also coincides with the 1985 Mexico City earthquake and 1986 aftershock suggesting that the 1985 fault rupture is also accumulating stress.

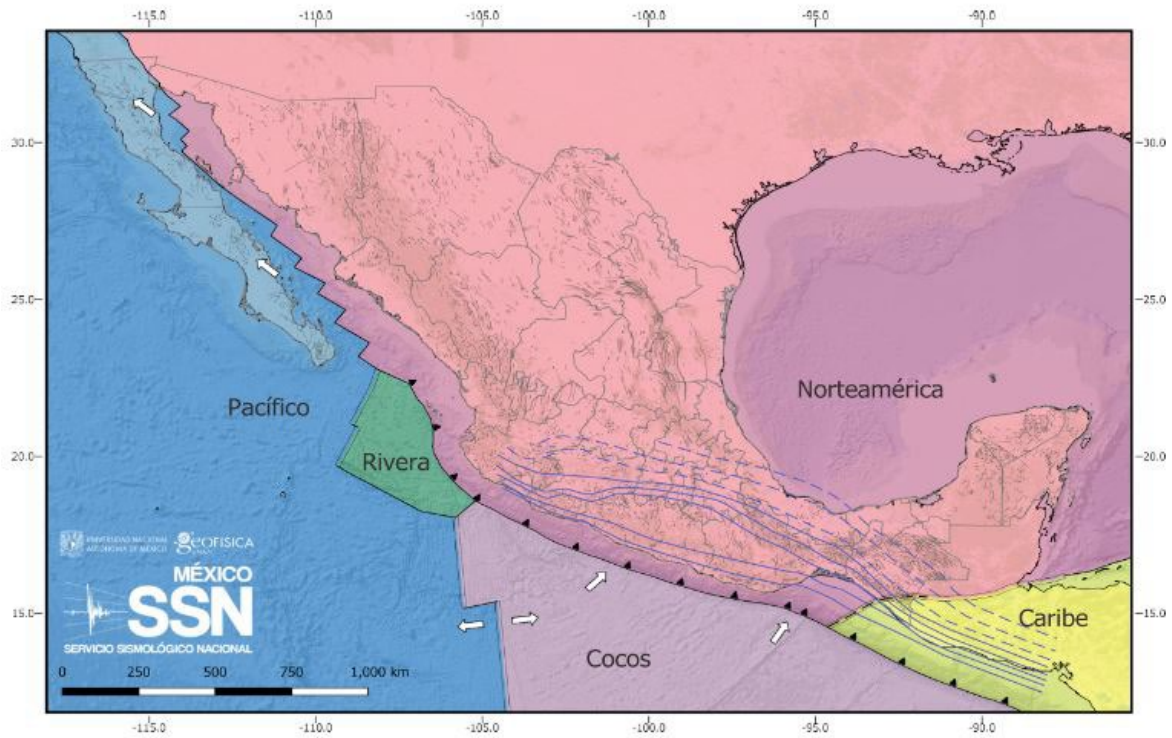


Figure 4. Plate tectonic map of Mexico (SSN, 2022)

Figure 5 presents the estimated intensity map by the Seismic Instrumentation Unit from the Institute of Engineering at National Autonomous University of México, UIS-IIUNAM, (UIS, 2022). The maximum intensities were presented in a rural, unpopulated area of the Mexican coast.

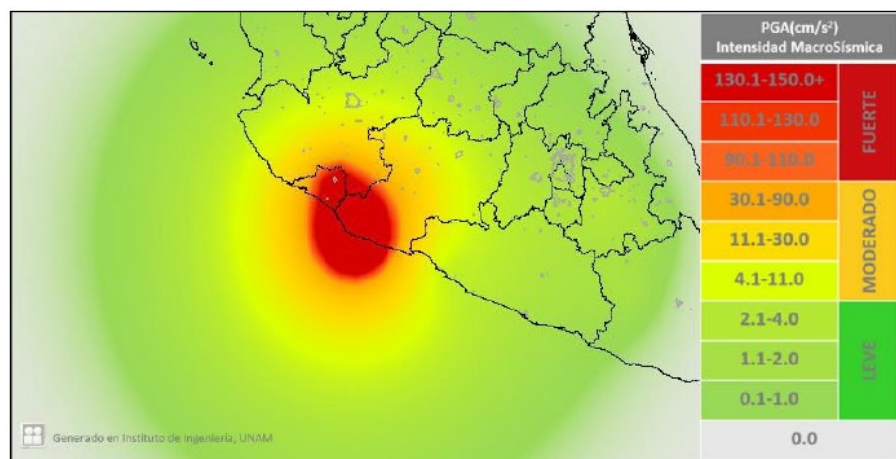


Figure 5. Estimated Intensity Map (UIS, 2022)

2.1 Tsunami Hazard

According to the National Mareographic Service, operated by the Institute of Geophysics of the National Autonomous University of Mexico (SMN-UNAM, 2022), which maintains a constant monitoring of the sea level on the coasts of Mexico. The September 19, 2022 earthquake created a tsunami that was recorded at the Puerto Vallarta, Manzanillo, Lázaro Cárdenas, Zihuatanejo and Acapulco API stations (Figure 6). No damage or injuries were reported as a result of the recorded tsunami.

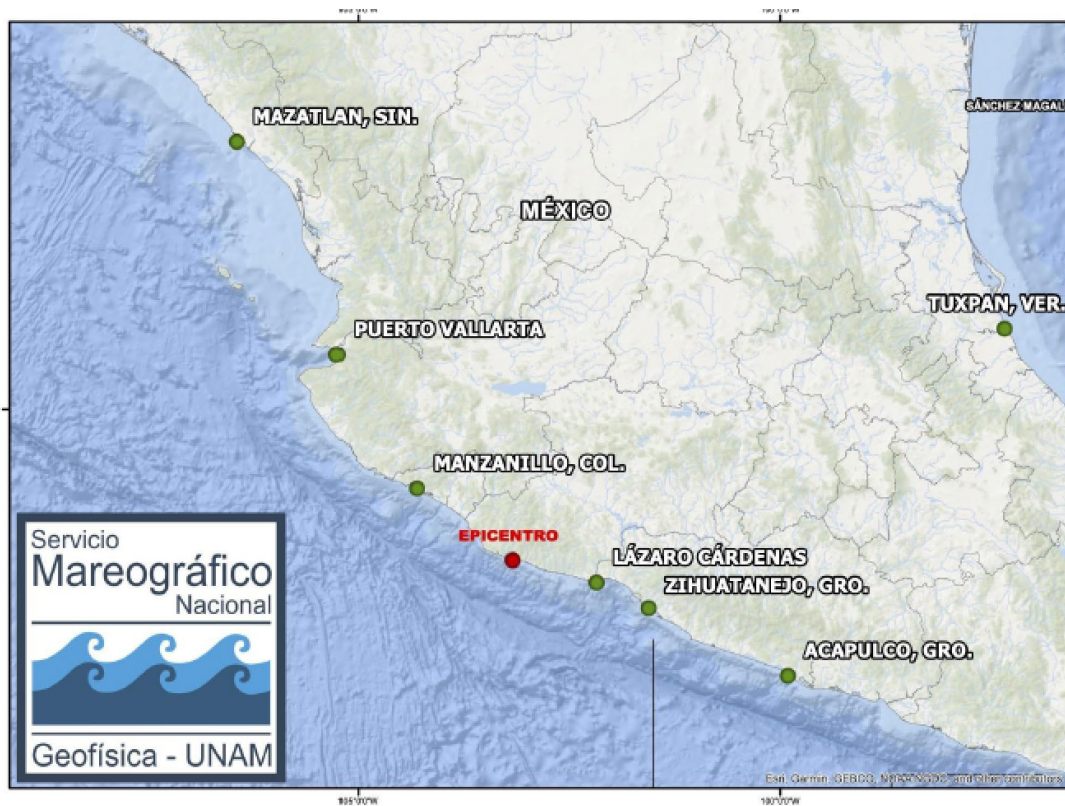


Figure 6. Map showing the location of the epicenter of the earthquake in red, and the nearby wave monitoring stations of the National Mareographic Service.

Manzanillo was the station where the most significant peak-to-peak amplitude of tsunami waves was recorded, with a magnitude of 1.75 m, followed by the stations of Zihuatanejo with 1.0 m, Acapulco with 0.63 m, Lazaro Cardenas with 0.42 m and Puerto Vallarta with 0.41 m. The station that first recorded the tsunami was Puerto Vallarta, just 5 minutes after

the earthquake, followed by Lazaro Cardenas, which received the first waves 10 minutes after the earthquake, Manzanillo 21 minutes later, Zihuatanejo 31 minutes later and finally Acapulco, which recorded the first tsunami waves 43 minutes after the earthquake occurred. Figure 6 presents the sea level recorded at the stations of the National Mareographic Service located in the Pacific Ocean, in the which some disturbance associated with the tsunami was noted. The horizontal axis corresponds to the time and the vertical axis to the wave heights, where each rectangle represents 10 cm. The vertical dotted line in red corresponds to the origin time of the earthquake.

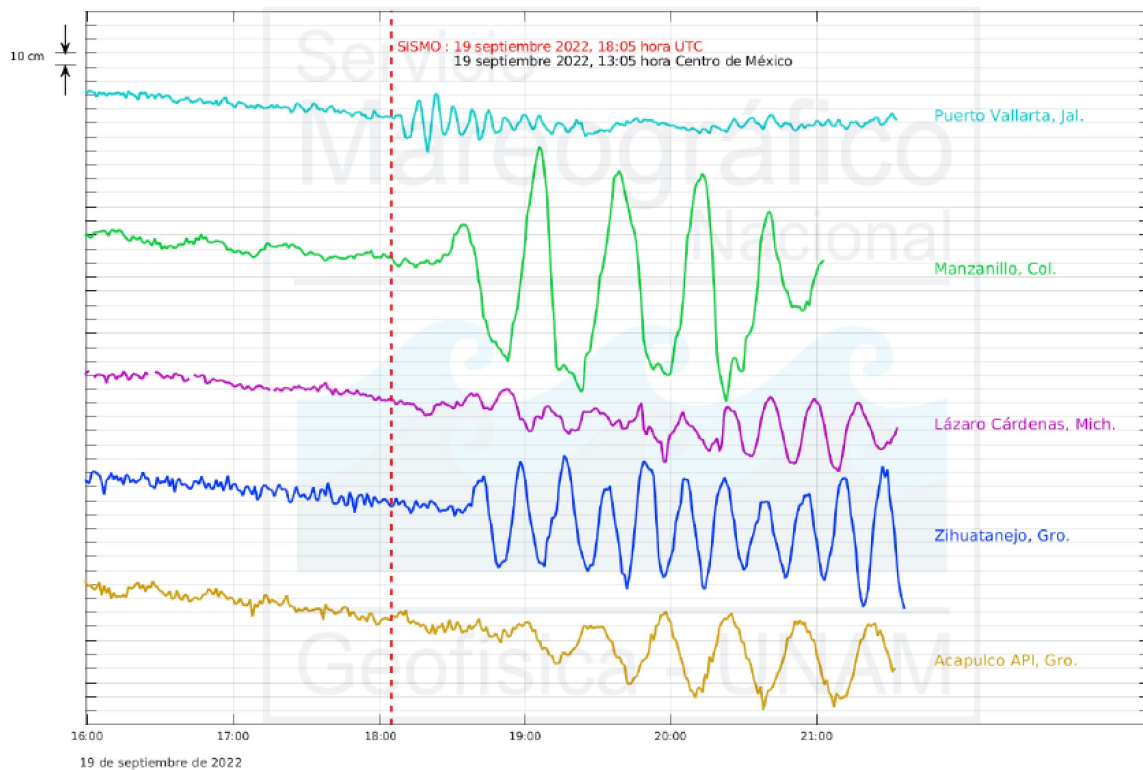


Figure 7. Sea level recordings following the September 19, 2022, earthquake at the stations monitored by the National Mareographic Service located along the west coast of Mexico.

2.2 Regional Geology

The following regional geology descriptions correspond to the central coast of western Mexico and portions of Jalisco, Colima, and Michoacan states surveyed by the research team.

The coastal areas of the state of Jalisco, south of Puerta Vallarta, are underlain by intrusive igneous rocks comprised of granite and granodiorite (KsGr-Gd; Figure 8). These coarse

grained granitics are often deeply weathered and saprolitic in the upper several to tens of meters of the ground surface. Granitic core stones up to several meters in size are often a residual weathering product of the saprolite that forms in the wet tropical climate.

The coastal region of the states of Colima and Michoacan can be characterized by the predominance of recent poorly consolidated materials like polymictic conglomerate and sandstones of the Pleistocene (QptCgp-Ar), and by alluvium, residual soils, and fine sands of the Holocene (Qal, Figure 8). Likewise, there is an alternation with intrusive igneous rocks, principally granite and granodiorite (KsGr-Gd), and igneous pyroclastic materials like andesitic tuffs and breccias composed of subangular fragments of andesite welded in a sand-clayey matrix (Kapa-A, Kap-BvA, and KapceTa-Ar).

The central part of Colima state is covered by the Mexican volcanic belt, where the active Nevado de Colima and Colima volcanoes are located. The product of the volcanic activity are mostly basalts and andesites of the Quaternary (QhOA-B, QhoB-A) and pyroclastic flows (QPc) near Colima city. Further north, after descending of Nevado de Colima volcano, in Ciudad Guzmán, there is a presence of laterally extensive sedimentary alluvium composed of mostly unconsolidated sands. The geological configuration of the Colima and Michoacan states (SGM, 2002; SGM, 1999; SGM, 2000) is presented in Figure 8, with the route followed by the reconnaissance team.

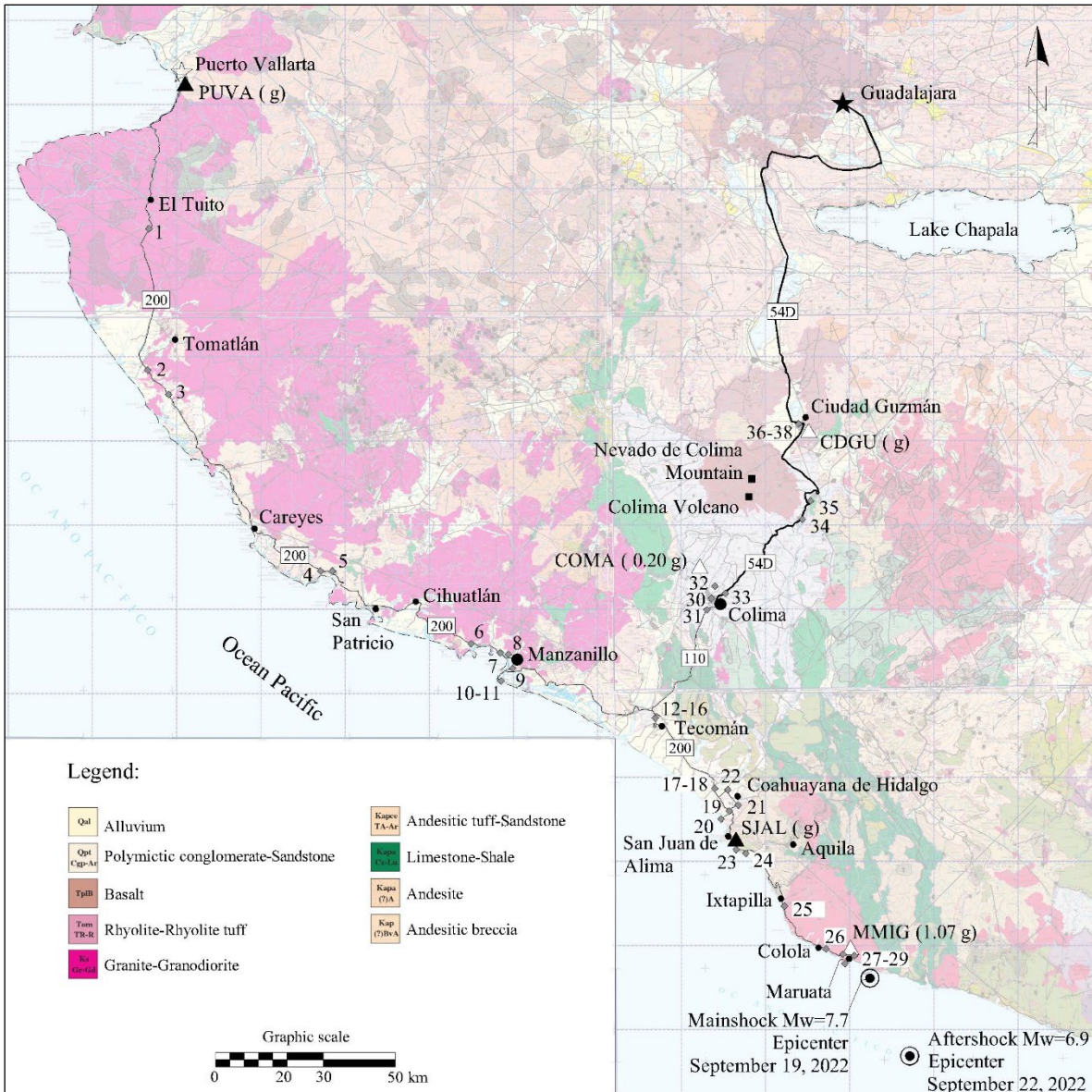


Figure 8. Geological map of the west-central coast areas of Mexico, (Modified from SGM, 2002; SGM, 1999; SGM, 2000).

As can be seen in Figure 8, the observed damage was mainly located in low lying, unconsolidated materials near the coastal area, where there is a predominance of loose to medium sands with a high saturation degree due to the low elevation and the presence of nearby water bodies.

3 STRONG GROUND MOTIONS

The M 7.7 event on September 19, 2022, generated several strong-motion recordings over a variety of geological site conditions, including free-field soil and rock as well as motions from various instrumented structures, which is summarized in Table 2 including the Peak Ground Accelerations (PGA). This information was provided by the UIS-IIUNAM. We recognize that epicentral distance is an inadequate distance metric for ground motion studies, but use this parameter in Table 2 due to the preliminary nature of this report and the current lack of availability of a finite fault model for this event.

Table 2. Strong motion recordings for the September 19, 2022, earthquake from the Institute of Engineering array. V_{S30} values estimated by Contreras (2022).

Station	Site type	V_{S30} (m/s)	Epicentral Distance (km)	PGA (cm/s ²)
MMIG	Rock	450	10	1067.3
COMA	Rock	475	74	199.45
ZIIG	Rock	425	141	5.1
CJIG	Rock	415	177	19.4
GDLC	Soil	230	214	24.1
ARIG	Rock	425	238	7.6
ATYC	Rock	700	257	2.9
ANIG	Rock	375	273	6.1
CAIG	Rock	700	280	1.6
IGIG	Soil	215	284	3.2
TOVM	Soil	230	318	5.2
ATVM	Rock	430	320	7.36
VNTA	Soil	215	239	1.38
DAIG	Rock	415	343	1.2
INVM	Soil	230	347	5.1
AOVM	Soil	215	353	9.5
AZVM	Soil	275	366	4.9
CCHN	Soil	220	367	5.1
CUP5	Rock	295	368	5.49
CMCU	Rock	475	368	5.5
ENP8	Rock	375	369	6.6
TLVM	Soil	225	369	7.5
TACY	Soil	350	369	6.7
CENA	Rock	450	370	7.1
PZCU	Rock	475	370	6.6
PZIG	Rock	475	371	6.1

4 DAMAGE OBSERVATIONS

The observations of damage presented hereafter correspond principally to the damage observed by the reconnaissance team at sites along and near the roads that connect the cities of Puerto Vallarta, Manzanillo, Tecoman, Maruata, Colima, Ciudad Guzman and Guadalajara, as is shown in Figures 2 and 8. Where damage is not reported along the route shown in Figure 2, damage was not observed (i.e., lack of discussion of damage for a traversed region indicates lack of damage, not lack of observation).

4.1 Structural Damage

Partial collapse of a roof top housing a gym in a four-story mall (Figure 9), occurred in Manzanillo, Colima. According to the National Emergency Committee, one person was killed in this building from the roof collapse. An adjacent building was affected as well but with minor damage. Two km away from this mall, collapse of masonry walls of a Coppel store were observed (Figure 10); apparently no punching or settlement occurred. A second story balcony failed near the harbor in Manzanillo (Figure 11). Additionally, damage to several perimeter masonry walls in Manzanillo were observed (some experienced total collapse and some tilting between 10-15°, see Figures 12 to 14). In the small towns further south, the number of damaged structures as well as their severity increased as they approached the epicentral area. A variety of structures were damaged by the earthquake but most damage appeared to be in taller buildings including hospitals, single-family buildings, hotels, and churches, which can be seen in Figures 15 to 27.



Figure 9. Collapse of roof in mall, Manzanillo, Colima, Waypoint Station 7 (Coordinates: 19.100552°, -104.325525°)

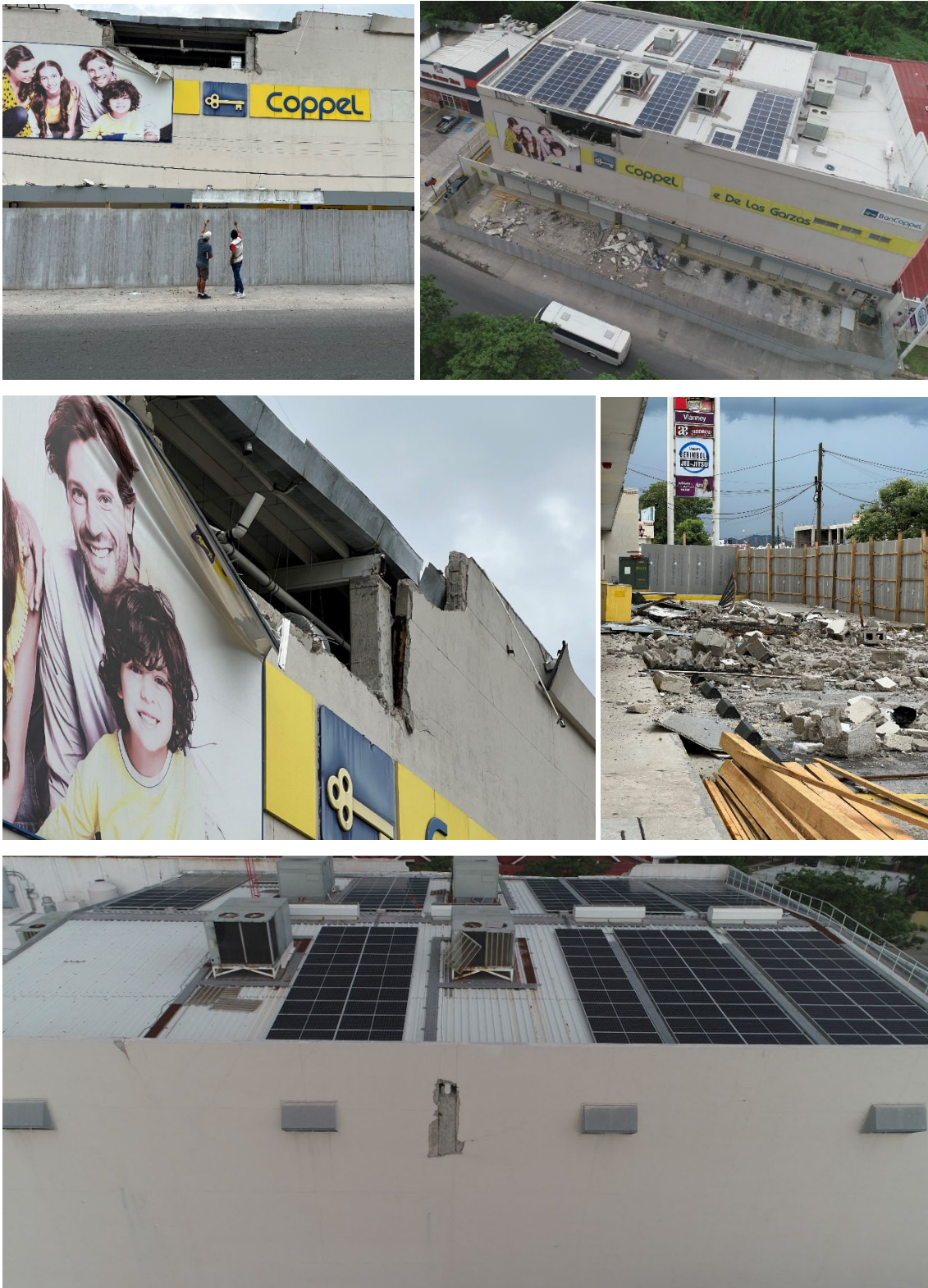


Figure 10. Collapse of third floor masonry walls of Coppel store, Manzanillo, Colima Waypoint Station 8 (Coordinates: 19.095606°, -104.302863°)



Figure 11. Partial collapse of balcony, Manzanillo, Colima
Waypoint Station 9 (Coordinates: 19.058136°, -104.290446°)

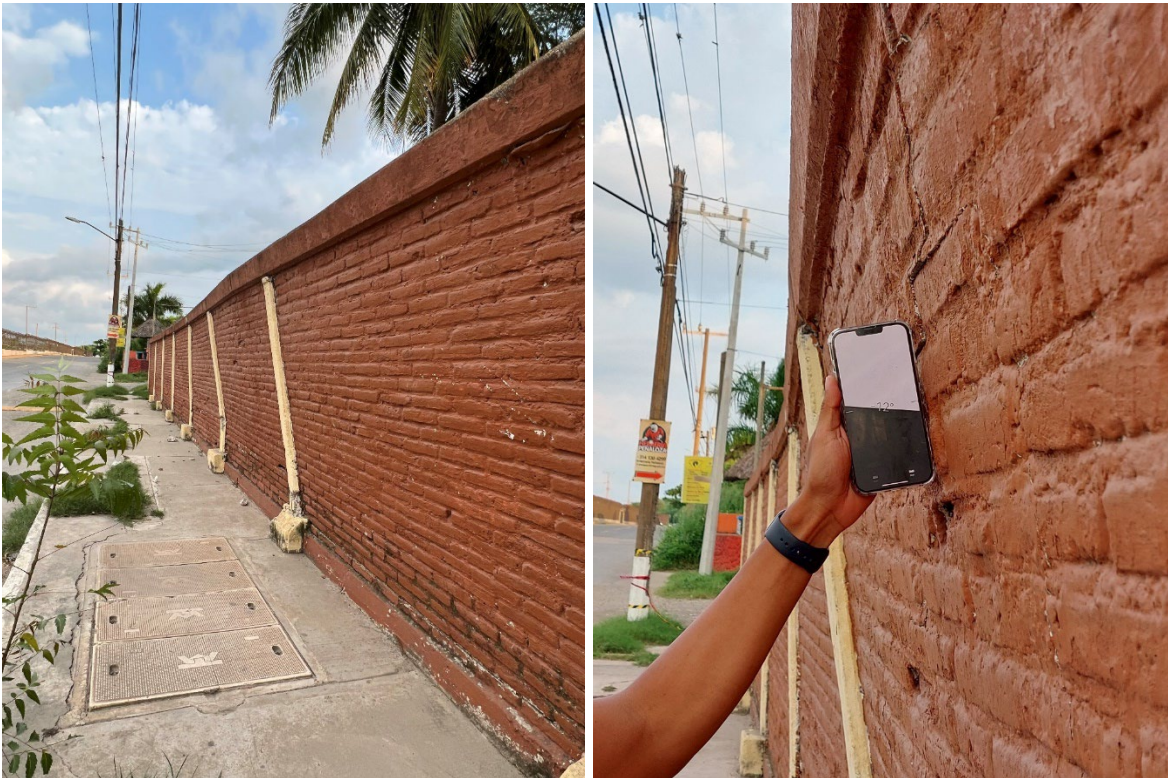


Figure 12. Column failures of perimeter walls of school, Manzanillo, Colima
Waypoint Station 10 (Coordinates: 19.024016°, -104.322869°)

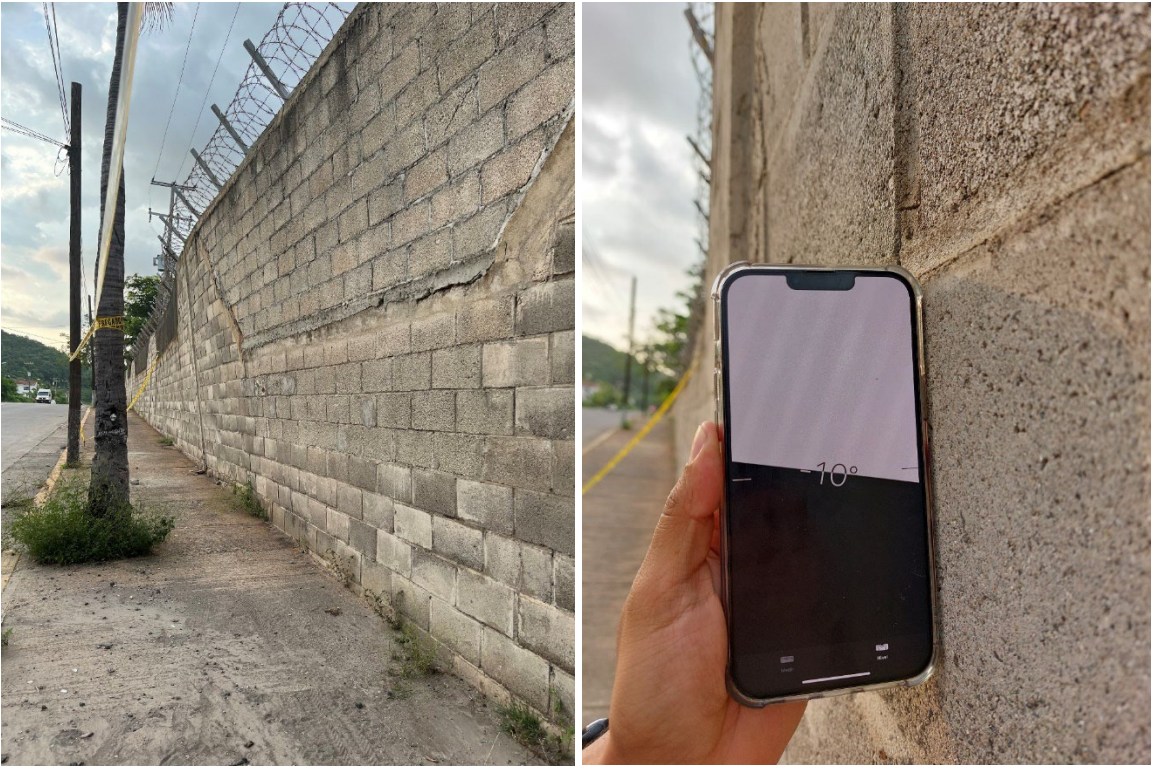


Figure 13. Columns failure of perimeter walls of thermal power station, Manzanillo, Colima, Waypoint Station 11 (Coordinates: 19.024788°, -104.323969°)



Figure 14. Collapse of perimeter wall of automobile workshop, Tecoman, Colima, Waypoint Station 12 (Coordinates: 18.918219°, -103.870195°)



Figure 15. Collapse of local grocery store, Tecoman, Colima
Waypoint Station 13 (Coordinates: 18.911143°, -103.871476°)



Figure 16. Column damage of supermarket, Tecoman, Colima
Waypoint Station 14 (Coordinates: 18.910863°, -103.871611°)



Figure 17. Damage in door frames and between structures, Tecoman, Colima
Waypoint Station 15 (Coordinates: 18.910531°, -103.87186°)



Figure 18. Damage to nonstructural elements in church, Tecoman, Colima
Waypoint Station 16 (Coordinates: 18.910498°, -103.87244°)



Figure 19. Total collapse of a two-story house with soft first floor, Coahuayana, Michoacan, Waypoint Station 22 (Coordinates: 18.728643°, -103.687277°)



Figure 20. Partial collapse of a court cover roof. Structure had evidence of severe rust, Colola, Michoacan. Waypoint Station 26 (Coordinates: 18.298116°, -103.412856°)



Figure 21. Collapse of masonry walls and damage to structural elements in community hospital and damaged column and wall of nearby masonry two story building, Maruata, Michoacan. Waypoint Station 28 (Coordinates: 18.27409°, -103.348231°)



Figure 22. Damage and slight cracking in non-structural elements of multiple buildings in the center of the city, Colima, Colima. Waypoint Station 30 (Coordinates: 19.243584°, -103.728062°)



Figure 23. Cracking on non-structural elements with damage on the corner columns, Colima, Colima. Waypoint Station 32 (Coordinates: 19.275421°, -103.716969°)



Figure 24. Vertical cracking in building, Colima, Colima.
Waypoint Station 33 (Coordinates: 19.255976°, -103.687608°)

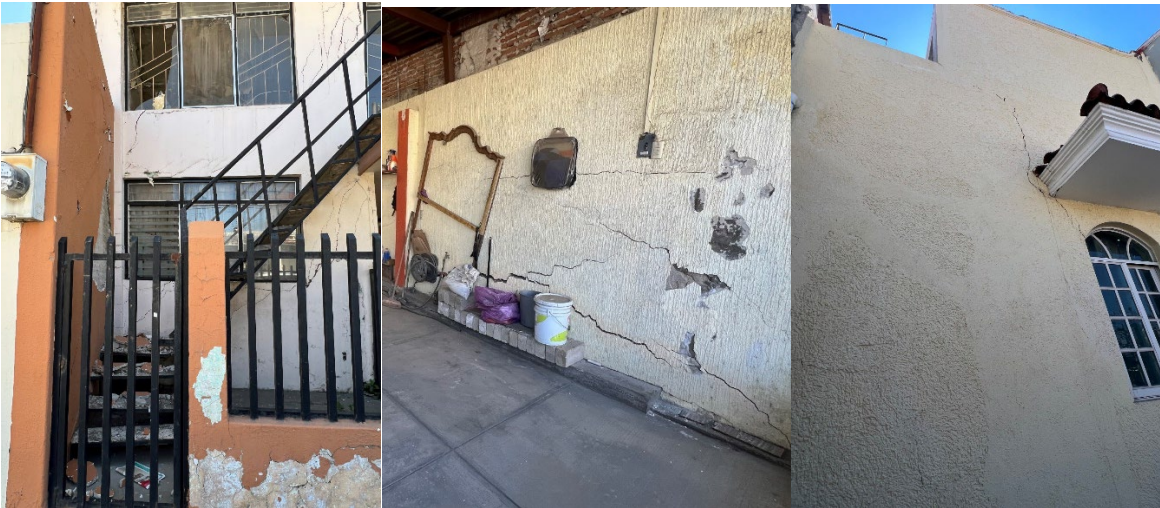


Figure 25. Severe damage in three continuous houses with extensive cracking on walls, floor lifting, and tilt of columns, Ciudad Guzman, Jalisco.
Waypoint Station 36 (Coordinates: 19.709474°, -103.467275°)



Figure 26. Roof cracking on church, Ciudad Guzman, Jalisco. Waypoint Station 37 (Coordinates: 19.703666°, -103.463191°)



Figure 27. Partial collapse and cracking of perimeter wall of local stadium, Ciudad Guzman, Jalisco. Waypoint Station 38 (Coordinates: 19.702541°, -103.471109°)

4.2 Road and Highway Damage

Minor damage in the form of cracking was noted along roads and highways within 50 km of the epicenter. Near the epicenter in Maruata, Michoacan, severe longitudinal cracking was detected on the road due to lateral movement. On average, the observed cracks were 6 m long, 38 cm wide, and 100 cm deep. Figure 28a depicts the road conditions before the earthquake; Figure 28b shows the conditions observed by the reconnaissance team.



Figure 28a. Road before the earthquake, (Google Earth, image date: May 2022).
(Coordinates: 18.282195°, -103.358294°)



Figure 28b. Severe longitudinal cracking on road due to lateral expansion, Maruata, Michoacan. Waypoint Station 27 (Coordinates: 18.282195°, -103.358294°)

4.3 Bridge Damage

Several cases of bridge damage were observed and are shown in Figures 29 to 34, along the route from Puerto Vallarta to Maruata (epicenter zone). The observed damage was mostly related to the opening of joints in decks of the bridges (typical gap of joints was about 6 to 10 cm wide), vertical cracking in abutments, lateral displacements of decks, and cracks in pier caps. All the damaged bridges were in operation, and only the bridges located in El Ticuiz, Michoacan, and Colima City, Colima, were undergoing repair work that was initiated after the earthquake.



Figure 29. Gap of joints in decks of the bridge and lateral displacements, Campo Acosta, Jalisco.

Waypoint Station 3 (Coordinates: 19.794496°, -105.263413°)



Figure 30. Gap of joints in decks of the bridge, Boca de Iguanas, Jalisco.
Waypoint Station 4 (Coordinates: 19.321026° , -104.817072°)



Figure 31. Vertical cracking in abutment of bridge, Boca de Iguanas, Jalisco.
Waypoint Station 6 (Coordinates: 19.125082° , -104.407973°)



Figure 32. Lateral displacements of decks and damage in pier caps of bridge, Arturo Noriega Pizano, Colima. Waypoint Station 17 (Coordinates: 18.72438°, -103.722248°)



Figure 33. Lateral displacements of decks with damage in pier caps of the bridge and rotational failure of abutment, El Ticuiz, Michoacan. Waypoint Station 19 (Coordinates: 18.670031°, -103.681472°)



Figure 34. Lateral displacements of decks and damage in pier caps of bridge, Colima, Colima. Waypoint Station 31 (Coordinates: 19.213032°, -103.739473°)

4.4 Culvert Damage

Damage to the sewer culvert, shown in Figure 35, was observed in Coahuayana, Michoacan. The damaged culvert was made of stones in mortar packed with fine materials. On average, the culvert was 8 m long, 4 m wide, and exhibited an artificial fill cover of approximately 1 m. The partial collapse of the entrance of the culvert affected the road to the center of town.



Figure 35. Collapse of the entrance of culvert made of masonry, Coahuayana, Michoacan. Waypoint Station 21 (Coordinates: 18.684114°, -103.669303°)

4.5 Landslides and Rockslides

Landsliding consisted of primarily shallow rockslides and rockfalls of bedrock material in road cuts adjacent to the federal highways along the reconnaissance route. Less frequent translational landslides were observed in natural slopes within bedrock hillsides near the epicentral area (~50 km radius). One long runout debris flow (hundreds of meters long) feature was noted at distance near Las Brisas, Michoacan. Numerous fresh rockfalls were observed in the epicentral area at nearly every cut slope along the federal highway. These rockfalls varied in size and were estimated at between 30 to 3000 cubic meters in volume.

The figures shown below are representative of the type and style of failures found in different areas along the reconnaissance route. Figure 36 shows a shallow earthflow of deeply weathered (saprolite) granitic bedrock containing large core stones (1-3 m) adjacent to the federal highway in El Cono, Jalisco. Figure 37 shows a wedge failure in jointed volcanic rock. Figure 38 was taken by a UAV near Las Brisas, Michoacan in the epicentral area and Figure 39 is from this same area. These rockslides and rockfalls originated in both natural and cut slopes adjacent to the federal highway. These failures did not appear to be re-activations of earlier failures but rather new slides. The estimated volumes of material involved in most of these rockslides and rockfalls was several thousand cubic meters each. According to the National Emergency Committee, in the states of Colima and Michoacan, landslide and rockslide debris on the roadways caused significant traffic delays and road closures, and clearing of the roadways and federal highways took several days to over a week in some cases.



Figure 36. Rockfalls on cutting slope along the road, El Cono, Jalisco.
Waypoint Station 1 (Coordinates: 20.240086°, -105.320644°)



Figure 37. Rock wedge failure on cutting slope along the road, La Cumbre, Jalisco.
Waypoint Station 2 (Coordinates: 19.860358°, -105.323112°)



Figure 38. Multiple rockfalls and landslides on cutting slopes along the road, Las Brisas, Michoacan. Waypoint Station 23 (Coordinates: 18.566463°, -103.65394°)



Figure 39. Rockfalls near Las Brisas, Michoacan. Waypoint Station 24 (Coordinates: 18.563754°, -103.646552°)



Figure 40. Rockfalls on cut slope along the road, Pialla, Jalisco. Waypoint Station 34 (Coordinates: 19.452558°, -103.469476°)

4.6 Soil Liquefaction

Evidence of liquefaction was noted in La Zapotera, El Ticuiz, Ixtapilla, and Maruata in the states of Colima and Michoacan. Liquefaction was demonstrated by lateral spreading features as well as sand boils and sand blows along open fissures. These effects are shown in Figures 41 to 44. The liquefaction was preceded near the coast in beach sands, along riverbeds, and natural levees. Lateral spreading occurred at sites with a natural slope or a nearby free face. A social media (Twitter, 2022) video was posted immediately after the earthquake in Coahuayana, Michoacan, about 50 km northeast of the epicenter, where a beach had been shattered into numerous elongate fractures and fissures stretching several hundred meters parallel to the coast (Figure 46). The feature was interpreted as caused by lateral spreading of the beach sands. The reconnaissance team used the UAV to look along the stretch of beach where the failure occurred, but these perishable features had been eroded by the incoming tides and waves prior to our visit. However, numerous other lateral spread features were observed further south along the same beach (Figure 43). Failure of a natural levee due to lateral spreading was found in La Zapotera, Colima (Figures 41 and 42). The lateral extent of the affected area is shown on Figure 42, in which red hash marks cracks and lateral displacement. The lateral displacement created an open graben near the head of the failure that had a lateral displacement of about 67 cm and vertical displacement of around 60 cm.

The cumulative lateral displacement of the slope was on the order of two meters. The lateral spread did not appear to affect the nearby bridge.

Sand boils or sand volcanoes were observed in a riverbed levee near Ixtapilla, Michoacan (Figure 44). The sand was ejected from points along a linear natural levee and buried nearby vegetation. There were over a dozen sand boils total, all with similar volumes of ejecta (<1 cubic meter). Fissures were evident near the sand boils but no ejecta from the fissures was observed.

Sand blows along fissures were observed along a back beach in Maruata, Michoacan (Figure 45). The fissures covered an area of approximately 200 sq. m and were on the order of 5 to 10 m long with lateral displacements of 5 to 15 cm. Sand ejecta was noted as having flowed from several of the fissures. Locals reported sand ejecta spouting as high as 1-2 m and continuing well beyond the duration of earthquake shaking.

There were no observations or reports of significant soil liquefaction affecting structures.



Figure 41. Lateral spread feature affecting a road along a natural levee, La Zapotera, Colima. Waypoint Station 18 (Coordinates: 18.717472°, -103.716876°)



Figure 42. Lateral spread feature from Figure 41, La Zapotera, Colima. Red hash marks note cracks and lateral displacement of affected area. Waypoint Station 18 (Coordinates: 18.717472°, -103.716876°)



Figure 43. Lateral spreading in beach sands due to liquefaction, El Ticuiz, Michoacan. Waypoint Station 20 (Coordinates: 18.653076°, -103.700458°)



Figure 44. Sand boils (sand volcanoes) in a riverbed. The sand was ejected from points along a linear natural levee and buried nearby vegetation, Ixtapilla, Michoacan. Waypoint Station 25 (Coordinates: 18.41615°, -103.532373°)



Figure 45. Lateral spreading and cracking in rural roads due to liquefaction, Maruata, Michoacan.

Waypoint Station 29 (Coordinates: 18.268759°, -103.350911°)



Figure 46. Lateral spreading in beach deposits near Coahuayana, Michoacan immediately after the earthquake (Twitter, 2022). These perishable features were eroded by the tide and waves prior to our visit.

4.7 Effects on Lifelines

The performance of pipelines and utilities (i.e., electrical power) was significantly affected during this event. The Federal Commission of Power, CFE, informs that the seismic event affects more than 1.2 million users in 5 states: Mexico City, the State of Mexico, Michoacan, Colima and Jalisco (CFE, 2022). The affected people represented 8% of the total users of the mentioned states. Table 3 presents the affected users for each state:

Table 3. Total affected users for state

State	Affected users
Mexico City	572,663
State of Mexico	335,938
Michoacan	106,037
Colima	145,808
Jalisco	72,055

REFERENCES

CFE, 2022. Boletín de prensa 19 de septiembre de 2022. CFE-BP-166/22. Comisión Federal de Electricidad

CNPC (2022). Informe de Coordinación Nacional de Protección Civil. Gabinete de Seguridad (in Spanish).

Contreras, V. (2022). Characteristics of Subduction Zone Ground Motions with an Emphasis on Latin America, Ph.D. Dissertation, UCLA.

History (2009). 1985 Mexico City earthquake. <https://www.history.com/topics/natural-disasters-and-environment/1985-mexico-city-earthquake>

Miranda, E. Abuchar, V. Alcocer, S. Aldea, S. Álvarez, J. Archbold, J. Arroyo, O. Arteta, C. Ballinas, E. Benavides, D. Blandón, C. Bravo, M. Caballero, J. Carrillo, J. Cruz, C. Espinoza, U. Gil, P. Guerrero, H. Gunay, S. Heresi, P. Lubin, C. Mayoral, J. Miranda, S. Pájaro, C. Piscal, C. Rivera, J. Rodríguez, V. Urango, A. Vargas, J. Velasco, L. (2022) "PRELIMINARY VIRTUAL RECONNAISSANCE REPORT (PVRR)", in AQUILA, MICHOACÁN, MEXICO SEPTEMBER 19, 2022, Mw 7.6 EARTHQUAKE. DesignSafe-CI. <https://doi.org/10.17603/ds2-sbcj-nx44> v1

SMN-UNAM (2022). Reporte rápido: Registro en las estaciones del Servicio Mareográfico Nacional del tsunami producido por el sismo de magnitud 7.7 ocurrido en Michoacán, Grupo de Trabajo del Servicio Mareográfico Nacional, Instituto de Geofísica, Universidad Nacional Autónoma de México, México. URL: <http://www.mareografico.unam.mx>

SSN (2022): Servicio Sismológico Nacional, Instituto de Geofísica, Universidad Nacional Autónoma de México, México. URL: <http://www.ssn.unam.mx>

Twitter (2022). (<https://twitter.com/AlertaCambio/status/1572666203000258562?s=20>)

UIS (2022). Sismo del 19 de septiembre de 2022, Coalcoman, Mich, México (M7.4), 13:05:09 Hora Local. REPORTE PRELIMINAR, Parámetros del Movimiento del Terreno

Wartman, J. and others, 2003, Preliminary Reconnaissance Report on the Geotechnical Engineering Aspects of the January 21, 2003 Tecoman (Colima), Mexico Earthquake, Geotechnical Extreme Events Reconnaissance (GEER), GEER-008 report, doi:10.18118/G6G592